npg

ORIGINAL ARTICLE

PSD-95 regulates D$_1$ dopamine receptor resensitization, but not receptor-mediated Gs-protein activation

Peihua Sun[1,*], Jingru Wang[1,*], Weihua Gu[1,*], Wei Cheng[2], Guo-zhang Jin[1], Eitan Friedman[3], Jie Zheng[2], Xuechu Zhen[1]

[1]State Key Laboratory of Drug Research, Department of Neuropharmacology, Shanghai Institute of Materia Medica, Chinese Academy of Sciences, Shanghai 201203, China; [2]Department of Physiology and Membrane Biology, University of California School of Medicine, Davis, CA 95616, USA; [3]Department of Physiology & Pharmacology, CUNY Medical School at CCNY, New York, NY, USA

The present study aims to define the role of postsynaptic density (PSD)-95 in the regulation of dopamine (DA) receptor function. We found that PSD-95 physically associates with either D$_1$ or D$_2$ DA receptors in co-transfected HEK-293 cells. Stimulation of DA receptors altered the association between D$_1$ receptor and PSD-95 in a time-dependent manner. Functional assays indicated that PSD-95 co-expression did not affect D$_1$ receptor-stimulated cAMP production, Gs-protein activation or receptor desensitization. However, PSD-95 accelerated the recovery of internalized membrane receptors by promoting receptor recycling, thus resulting in enhanced resensitization of internalized D$_1$ receptors. Our results provide a novel mechanism for regulating DA receptor recycling that may play an important role in postsynaptic DA functional modulation and synaptic neuroplasticity.
Keywords: PSD-95, dopamine receptor, Gs-protein activation, desensitization, recycling, resensitization

Introduction

Dopamine (DA) receptors are members of the G-protein-coupled receptor family, which consists of five subtypes, namely, the D$_1$-like receptors, D$_1$ and D$_5$, and the D$_2$-like receptors, D$_2$, D$_3$ and D$_4$. In response to agonist binding, the DA receptors activate respective G-proteins, resulting in subsequent activation of second messenger systems. The activated DA receptor subsequently undergoes desensitization, internalization and resensitization [1, 2]. Agonist-mediated internalization is believed to be an important mechanism for discharging the bound receptors and making receptor sites available again on the surface of the cell membrane. Thus, studying receptor trafficking and its regulatory mechanisms is critical for understanding receptor function and regulation. It has been reported that, in response to stimulation, perisynap-

tic DA receptors undergo a different pattern of agonist-induced internalization compared with extrasynaptic DA receptors [3]. Considering the unique structure of postsynaptic density (PSD) and its role in the modulation of neurotransmission [4], it is reasonable to speculate that the PSD may play an important role in functional regulation of the DA receptor.

The PSD is enriched with PSD-95 protein. It is now clear that the PSD-95 family of proteins not only act as anchor proteins, but also function as important modulators of signaling [4, 5]. Abnormal PSD-95 expression has been implicated in Parkinson's disease and schizophrenia and is believed to contribute to abnormal neurotransmission in these diseases [6-8]. The direct association of PSD-95 with N-methyl-D-aspartate (NMDA) or other receptors was demonstrated to be an essential mechanism for PSD-95-regulated function of those neurotransmitter receptors [9-11]. In addition, PSD-95 associates with adhesion molecules, signaling enzymes and ion channels [12-16]. We recently reported that modulation of NMDA receptor function by D$_1$ receptor requires the presence of PSD-95. In the absence of PSD-95, D$_1$ receptors fail to regulate NMDA receptor function. We further demonstrated that PSD-95 physically associates with the D$_1$

*These three authors contributed equally to this work.
Correspondence: Xuechu Zhen
Tel: +86-21-50806750; Fax: +86-21-50806750
E-mail: xczhen@mail.shcnc.ac.cn

DA receptor [17]. A recent report also confirmed this association [18]. The present investigation aims to clarify the functional relationship between PSD-95 and D_1, as well as other DA receptors. Specifically, we examined the role of PSD-95 in D_1 receptor function and trafficking. Our results reveal a dynamic association of PSD-95 with the D_1 receptor in response to DA receptor stimulation. We demonstrated that this association did not alter D_1 receptor-stimulated cAMP production or Gs-protein activation, but significantly enhanced the resensitization of the D_1 DA receptor by accelerating D_1 receptor recycling to the cell membrane. The present study provides a novel mechanism for regulating DA receptor recycling that may play an important role in postsynaptic DA functional modulation and synaptic neuroplasticity.

Results

Both D_1 and D_2 DA receptors are physically associated with PSD-95

In HEK-293 cells co-expressing D_1 (HA-tagged) and PSD-95 (myc-tagged), PSD-95 was found in the D_1 receptor immunoprecipitates of anti-HA antibody (Figure 1A, left), suggesting that D_1 receptor physically interacts with PSD-95. Multiple control experiments indicate that the association of PSD-95 and D_1 receptor is specific (Figure 1A, right). This was further confirmed with FRET assays in HEK-293 cells that co-expressed D_1-CFP and PSD-95-YFP. Assessment of the fluorescence signal from the plasma membrane clearly showed FRET; the average FRET efficiency obtained from a total of 60 cells was $2.96 \pm 0.49\%$ (Figure 1B and 1C). Because D_1 is known to dimerize [19], we used cells co-expressing D_1-CFP and D_1-YFP as positive controls. FRET signals ($3.64 \pm 0.37\%$, $n = 45$) similar to those between D_1 and PSD-95 were observed, whereas no FRET signal was detected (FRET efficiencies of $0.02 \pm 0.78\%$, $n = 25$) from negative control cells in which D_1-CFP was co-expressed with the unrelated TRPV3 channel (TRPV3-YFP). Moreover, when the same FRET method was applied to cells expressing D_1-CFP alone, a FRET value of less than 0.01% was obtained, further confirming the reliability of the approach. In agreement with a previous report [18], we also demonstrated that all NT-containing domains of PSD-95 are able to support the interaction between D_1 receptor and PSD-95, regardless of truncations (Figure 1D). Taken together, our data suggest that the D_1 receptor associates directly with PSD-95. Remarkably, the direct interaction was not limited to the D_1 receptor and PSD-95 because we also found constitutive interactions between PSD-95 and the D_2 and D_5 DA receptors (Figure 1E). These data therefore indicate that PSD-95 interacts with both D_1-like and D_2 DA receptors.

Stimulation of D_1 receptors alters the interaction between D_1 receptor and PSD-95 in vitro and in vivo

To determine whether interaction between D_1 receptor and PSD-95 can be regulated by receptor activation, HEK-293 cells were transiently transfected with D_1-CFP and PSD-95-YFP. FRET signals were determined before and after DA treatment (10 μM). There was a significant increase in FRET signal (from $2.96 \pm 0.49\%$ to $6.87 \pm 1.16\%$; $P < 0.0005$) after 5 min of treatment with DA (Figure 2A). The results are consistent with the co-immunoprecipitation data. However, the enhanced association in response to D_1 receptor stimulation was transient because it rapidly returned to basal levels after 30 min (Figure 2B). This transient alteration of association was also observed *in vivo*. Administration of the D_1 receptor agonist, SKF38393 (i.p., 2 mg/kg), to rats significantly enhanced frontal cortical D_1 receptor-PSD-95 association measured at 8 min (2.07-fold, $P < 0.01$) and 16 min (1.64-fold, $P < 0.05$) (Figure 2C). This result indicates that D_1 receptor activation increases the association of brain D_1 receptor and PSD-95 *in vivo*.

PSD-95 does not alter D_1 receptor-stimulated cAMP production

We next studied whether the association between D_1 and PSD-95 alters D_1 receptor-stimulated cAMP production in response to DA stimulation. HEK-293 cells stably expressing D_1 receptors were transiently transfected with mock, full-length or truncated PSD-95; DA-stimulated cAMP accumulation was assessed. No significant stimulation of cyclase was detected with the full-length or truncated forms of PSD-95 (Figure 3A and Table 1), indicating that PSD-95 does not influence D_1 receptor activation. To further confirm this observation, we performed [^{35}S]GTPγS binding assays to detect DA-stimulated G-protein activation. No difference in G-protein activation in response to DA stimulation was noted in D_1 receptor/PSD-95 co-expressing cells (Figure 3B). This is further supported by the data obtained from saturation-binding analyses in which co-transfection of PSD-95 elicited no effect on membrane D_1 receptor-binding properties (K_d, 1.31 ± 0.16 vs 1.39 ± 0.18 nM; B_{max}, 10.67 ± 1.14 vs 10.59 ± 2.30 pmol/mg) (Figure 3C). Taken together, our data clearly indicate that PSD-95 does not alter D_1 receptor activation.

PSD-95 does not alter D_1 receptor desensitization, but enhances D_1 receptor resensitization

The results described in the above section indicate that PSD-95 does not affect D_1 receptor-stimulated cAMP
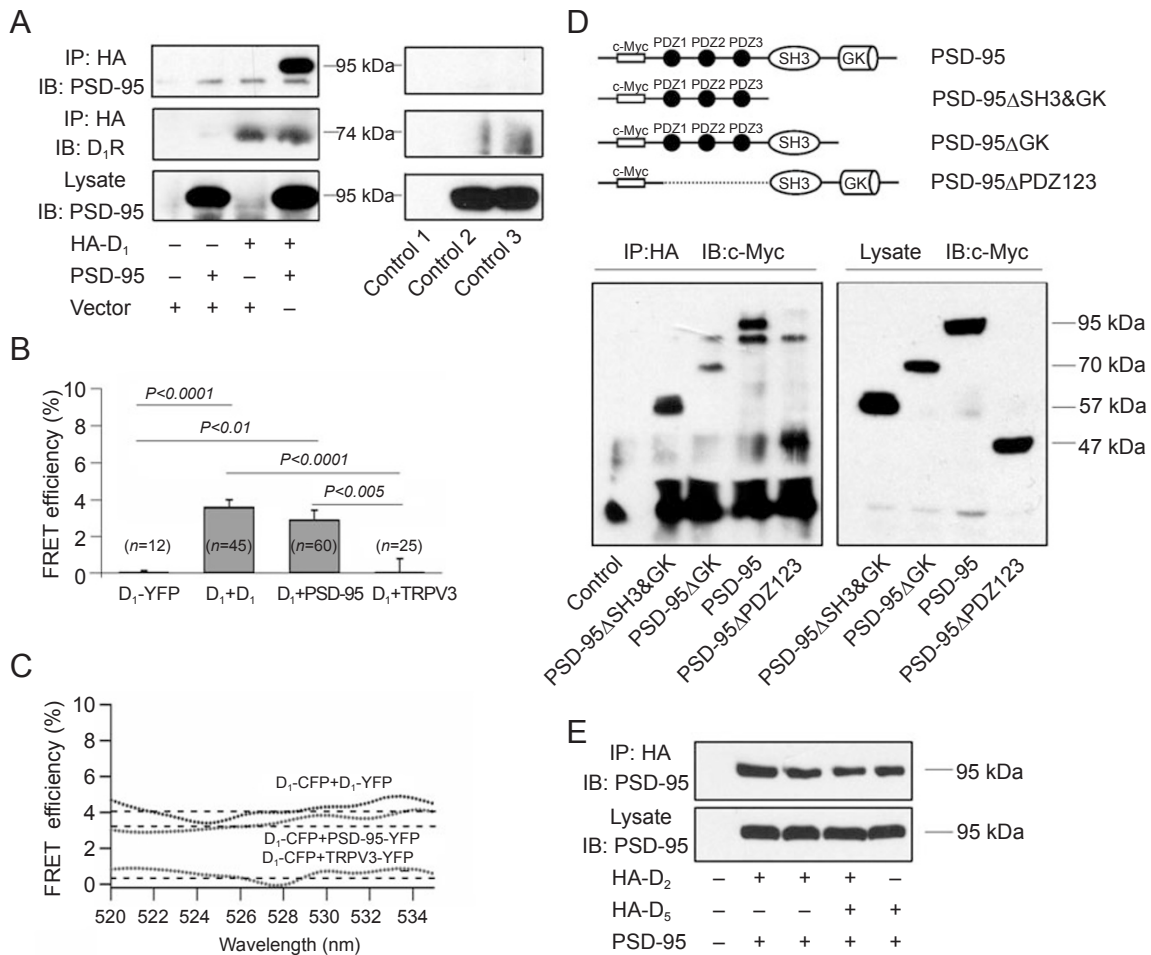
Figure 1 PSD-95 physically associates with DA receptors. **(A)** Left: HEK-293 cells were transfected with empty vector (lane 1), PSD-95 or D_1 receptor alone (lane 2 and 3) or co-transfected with D_1 receptor and PSD-95 (lane 4). Cell lysates were prepared and used for immunoprecipitation using anti-HA antibody, as described under Materials and Methods. The immunocomplex was resolved on SDS-PAGE and the membrane was blotted with anti-PSD-95 antibody (1:1 000) or anti-D_1R antibody (1:500). Expression of PSD-95 in cell lysates was also shown. Right: Multiple controls for the immunoprecipitation assay. Control 1: anti-HA antibody without cell lysate; Control 2: D_1/PSD-95 cell lysate without anti-HA antibody; Control 3: D_1/PSD-95 cell lysate + rabbit IgG. **(B)** Significant FRET signals were observed from HEK-293 cells co-expressing either D_1-CFP + D_1-YFP (positive control) or D_1-CFP + PSD95-YFP. FRET was not observed from cells that expressed D_1-YFP alone or co-expressed D_1-CFP + TRPV3-YFP (negative controls). **(C)** FRET efficiencies in relation to wavelength. A stable level of FRET was observed over a broad range of wavelengths. **(D)** HEK-293 cells stably expressing D_1 receptor (HA-tagged) were transfected with empty vector (lane 1), c-Myc-tagged PSD-95 or c-Myc-tagged truncated PSD-95 constructs (lanes 2~5). Immunoprecipitation and immunoblot were performed as described above. **(E)** HEK-293 cells stably expressing D_2 or D_5 receptor (HA-tagged) were transfected with PSD-95. Lane 1 shows HEK-293 cells transfected with empty vector. Cell lysates were prepared and used for immunoprecipitation using the anti-HA antibody. The presence of PSD-95 in anti-HA precipitates was then detected.

production; we wondered whether PSD-95 alters receptor desensitization and/or resensitization. Desensitization was assessed in HEK-293 cells stably expressing D_1 that were transiently co-transfected with mock, full-length or truncated PSD-95. The cells were treated with DA and washed prior to being challenged with DA for an additional 10 min to assess receptor desensitization. The cells

were then harvested for cAMP assay. As shown in Figure 4, DA-stimulated cAMP production was not changed by either PSD-95 or its truncated forms, clearly indicating that PSD-95 elicits no effect on D_1 receptor desensitization.

To assess resensitization, stable D_1-expressing HEK-293 cells were transiently co-transfected with mock, full-length (Figure 5A) or truncated forms of PSD-95 (Figure

A

B

C
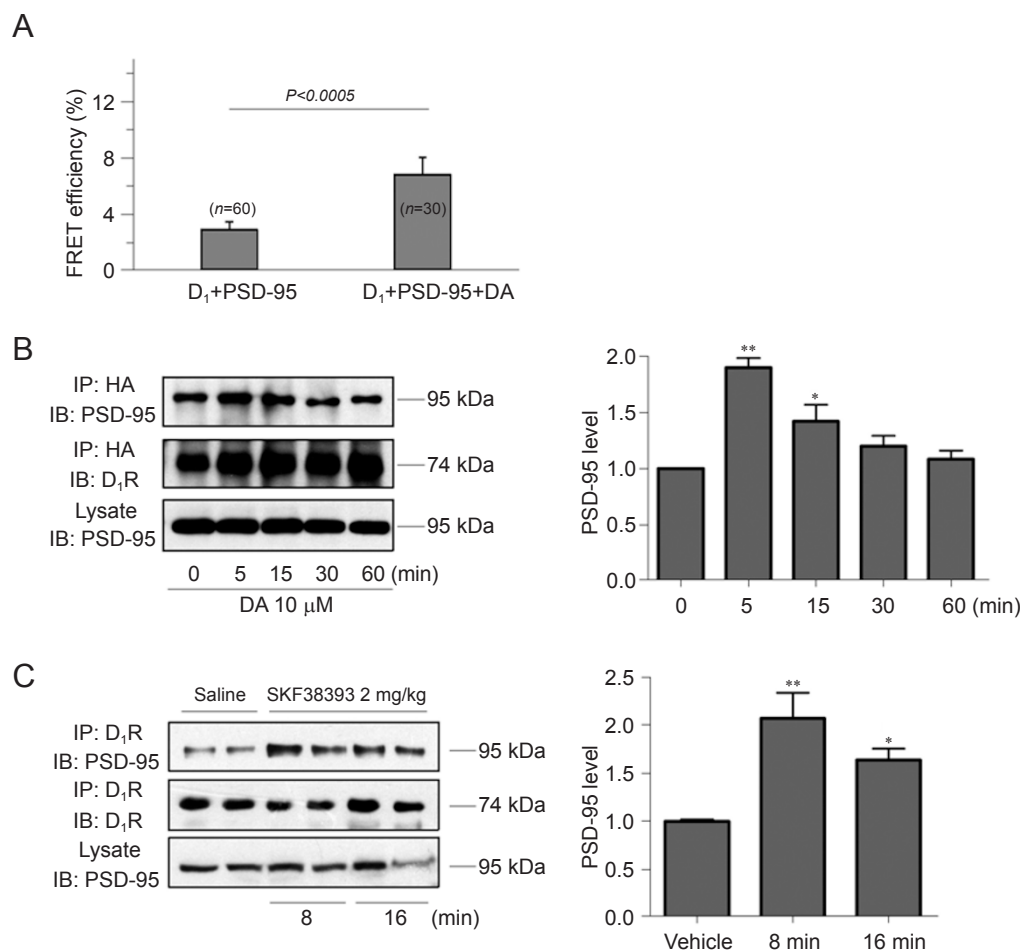
Figure 2 Dynamic changes to the D_1 receptor and PSD-95 interaction in response to D_1 receptor stimulation. **(A)** HEK-293 cells were transiently transfected with D_1-CFP and PSD95-YFP. Cells were then treated with 10 μM DA for 5 min prior to measurement of FRET efficiency. Treatment with DA significantly increased FRET efficiency, indicating that stimulation of the D_1 receptor enhanced its association with PSD-95. **(B)** The time course of association between D_1 receptors and PSD-95 in response to 10 μM DA stimulation in HEK-293 cells that were co-transfected with D_1-HA and PSD-95. **(C)** *In vivo* stimulation of D_1 receptors by SKF 38393 time dependently enhanced the association of D_1 receptor with PSD-95 in prefrontal cortex. SD rats ($n = 5$, each time point) received (i.p.) the selective D_1 receptor agonist, SKF38393 (2 mg/kg), for 8 or 16 min before sacrifice. The prefrontal cortex was then collected and lysed. D_1 receptor immunoprecipitation was performed as described using anti-D_1DR antibody; for Western blot anti-PSD-95 antibody (1:1 000) was used. Data are representative results from at least three independent experiments for **(B** and **C)**. Quantification of PSD-95 levels (shown in the bar graphs) was performed as described under Materials and Methods. ******$P < 0.01$, *****$P < 0.05$.

5B). Cells were pre-incubated with 10 μM DA for 1 h to induce receptor desensitization. The cells were washed three times and challenged at the designated times with DA for 10 min before measurement of cAMP. Figure 5A indicates that PSD-95 significantly enhanced D_1 receptor resensitization. A significant enhancement was already observed at 3 h ($P < 0.05$) following the initial 1-h DA treatment, and this enhancement increased further at subsequent time points (5 h, $P < 0.01$) compared with cells that were not co-transfected with PSD-95 (Figure 5A).

However, it was also noted that co-transfection with the PSD mutants failed to induce a change in D_1 receptor resensitization (Figure 5B). Thus, it appears that full-length PSD-95 is required for D_1 receptor resensitization.

PSD-95 accelerates membrane D_1 receptor recovery via enhancement of receptor recycling

To find out how PSD-95 enhances D_1 receptor resensitization, we examined the recovery of plasma membrane D_1 receptors. In this experiment, cells were subjected
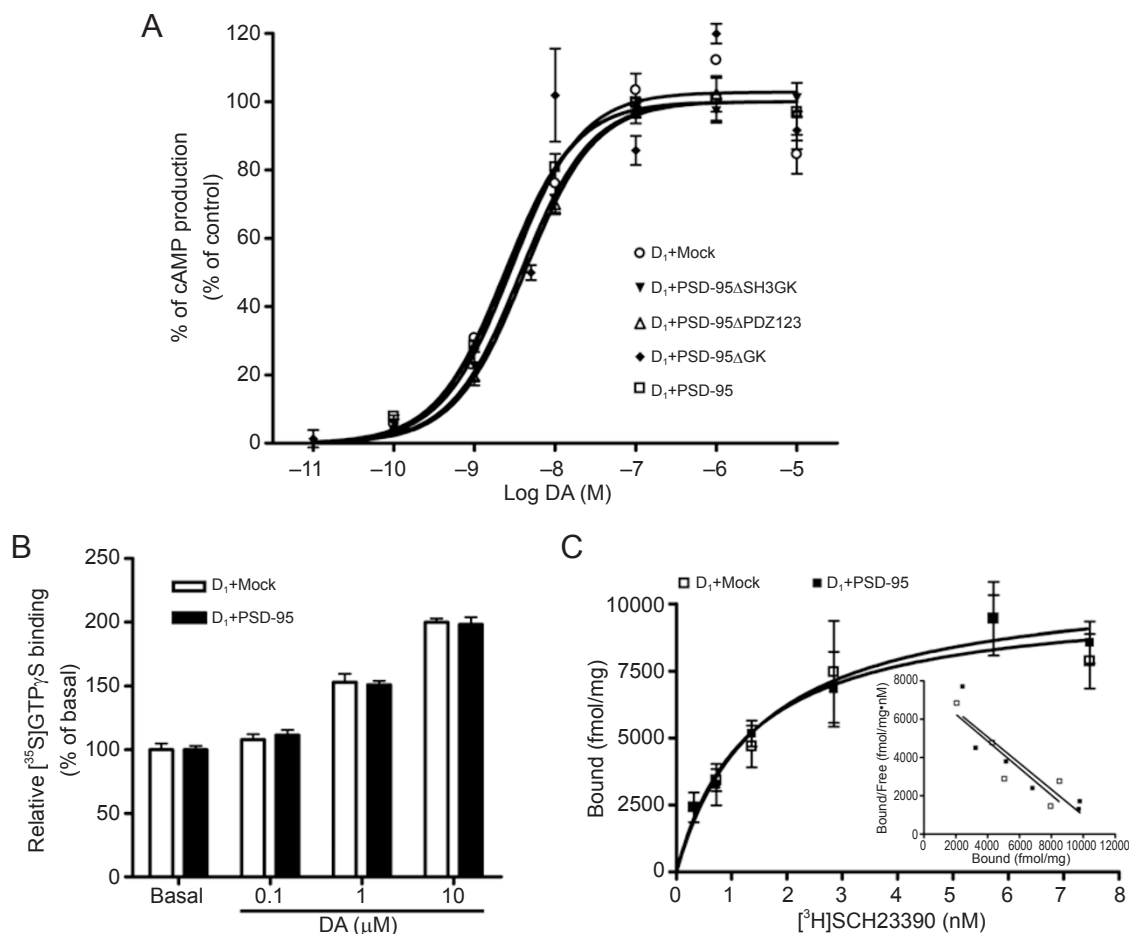
Figure 3 PSD-95 does not alter D_1 receptor-stimulated cAMP production and Gs-protein activation in cells co-expressing PSD-95 and D_1 receptor. **(A)** HEK-293 cells stably expressing D_1 receptors were transiently transfected with mock, full-length or mutant PSD-95. After 24 h of transfection, cells were incubated for 12 h in serum-free DMEM before various concentrations of DA were added for a period of 10 min. The cells were harvested for further assays. The cAMP content was determined as described under Materials and Methods. The EC_{50} and relative E_{max} values are shown in Table 1. **(B)** Cells were treated with various concentrations of DA for 10 min before harvesting. The [^{35}S]GTPγS binding assay was performed as described under Materials and Methods. Data are expressed as means ± SE for at least three independent experiments. **(C)** PSD-95 co-transfection did not alter D_1 receptor-binding properties. After 48 h of transfection, cell membranes were prepared for saturation-binding assays. The saturation binding of D_1 receptor in the membrane fraction was estimated using increasing concentrations of [^{3}H]SCH23390 (0.1-8 nM). The B_{max} and K_d were obtained by Scatchard analysis (inset) using data obtained from at least three independent experiments. B_{max}=10.67±1.14 and 10.59 ± 2.30 pmol/mg with corresponding K_d=1.31 ± 0.16 and 1.39 ± 0.18 nM for D_1-expressing cells and for cells co-transfected with D_1 and PSD-95, respectively.

to DA stimulation for 1 h to induce D_1 receptor internalization. The cells were then washed and cultured for 2, 6 or 15 h before cell collection and measurement of cell surface D_1 receptors was performed using the method described above. The density of cell surface D_1 receptors was reduced to 61.68 ± 9.06% in D_1 receptor-expressing cells and to 60.26 ± 12.36% in D_1 and PSD-95 co-expressing cells in response to 1-h DA stimulation compared with the respective control cells that were not exposed to DA. At 2 h after washing, D_1 DA recep-

tor density in the plasma membranes of D_1/PSD-95 co-expressing cells was significantly higher than that of cells expressing D_1 and mock (76.45 ± 7.21% vs 63.47 ± 9.88%). At 6 h after washing, the membrane receptors recovered to 98.49 ± 13.66% of control in D_1/PSD-95 co-expressing cells, which is significantly higher than that observed in membranes taken from cells without PSD-95 co-expression (53.15 ±19.61%). There was only 77.78 ± 4.91% recovery of D_1 receptors at the cell surface in D_1-expressing cells at 15 h after washing, whereas the full

Table 1 PSD-95 does not alter D_1 receptor-stimulated cAMP production

| Cell	Agonist potency $EC_{50} \pm SE$ (nM)	Agonist efficacy $E_{max} \pm SE$
D_1 + Mock	4.46 ± 0.51	1.00 ± 0.00
D_1 + PSD-95	5.08 ± 1.00 [NS]	1.05 ± 0.03 [NS]
D_1 + PSD-95ΔSH3GK	2.98 ± 0.75 [NS]	1.10 ± 0.05 [NS]
D_1 + PSD-95ΔGK	2.56 ± 0.34 [NS]	1.03 ± 0.01 [NS]
D_1 + PSD-95ΔPDZ123	3.92 ± 0.28 [NS]	1.01 ± 0.13 [NS]

HEK-293 cells stably expressing D_1 receptors were transfected with mock, full-length or truncated PSD-95. Thirty-six hours after transfection cells were treated with 10 μM dopamine for 10 min before harvest. The cAMP content assay was performed as described in "Materials and Methods" The results represent the average of three independent experiments. The EC_{50} and E_{max} relative values were analyzed using the Student's paired *t*-test (NS: no significant difference compared with cells expressing D_1 receptor alone).
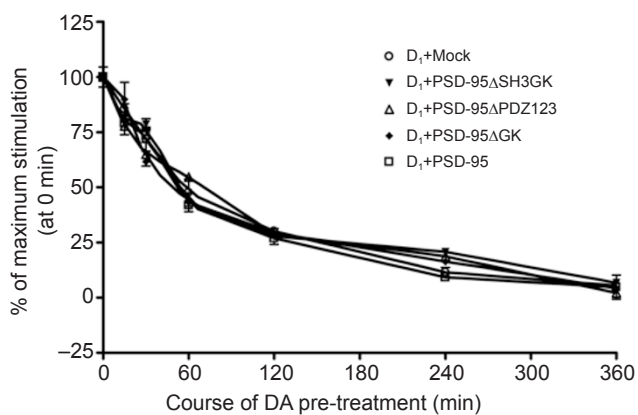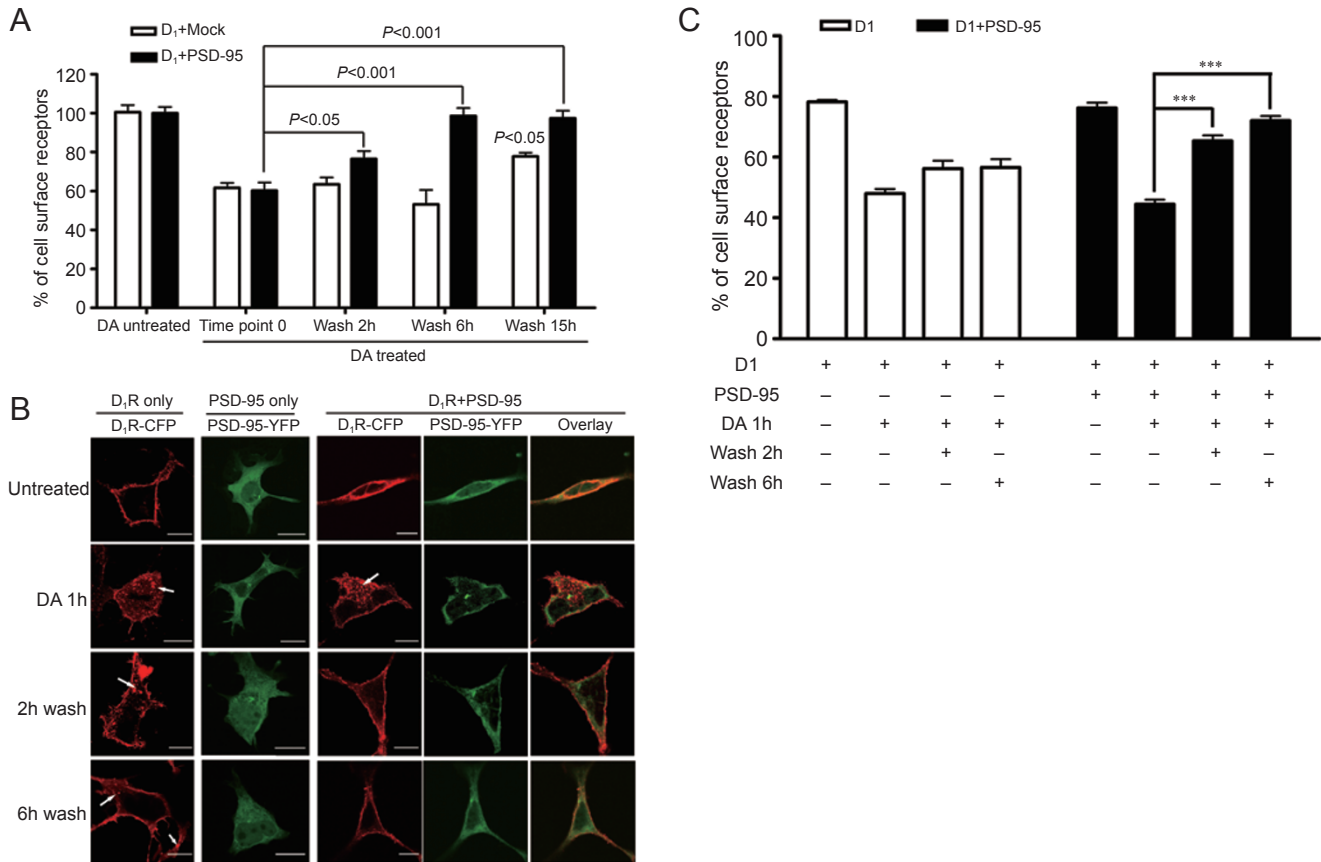

Figure 4 PSD-95 co-transfection does not alter D_1 receptor desensitization. HEK-293 cells stably expressing D_1 receptors were co-transfected with mock, full-length or mutant PSD-95. Cells were preincubated with 10 μM DA for 15, 30, 60, 120, 240 and 360 min. After being washed, cells were challenged with 10 μM DA for 10 min. The cAMP content was measured and expressed as a percentage of control (DA-stimulated cAMP in cells that were not subjected to desensitization treatment, time point 0). Data are the summary of three independent experiments.

focal microscopy at 2 and 6 h in cells co-expressing D_1 and PSD-95 (Figure 6B and 6C). Thus, PSD-95 enhances the trafficking of the D_1 receptor by accelerating the rate of recovery of receptors at the plasma membrane. PSD-95-enhanced D_1 receptor recovery was further supported by our observation that co-expressing PSD-95 with D_1 results in an increased spontaneous internalization of D_1 receptors in some unstimulated cells (Figure 6B, Row 1). However, this increased spontaneous internalization does not significantly alter the density of cell surface receptors (Figure 6A and 6C, DA untreated), suggesting
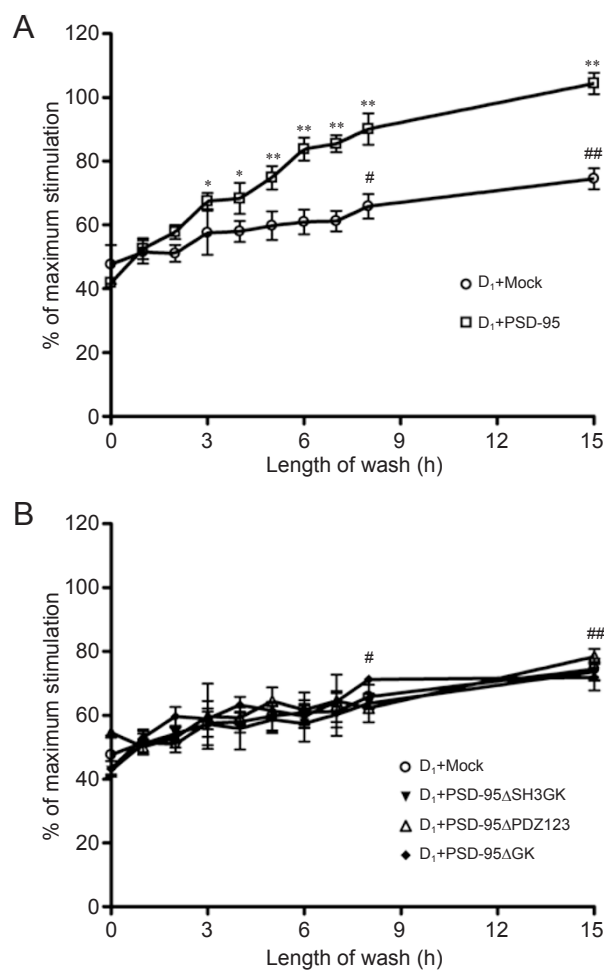
Figure 5 PSD-95 co-transfection enhances D_1 receptor resensitization. HEK-293 cells stably expressing D_1 receptors were co-transfected with mock or full-length PSD-95 **(A)** or PSD-95 mutants **(B)**. Cells were incubated with 10 μM DA for 1 h to induce D_1 receptor desensitization (time point 0). After being washed, cells were cultured in serum-free DMEM for the indicated number of times before 10 μM DA challenge for an additional 10 min. cAMP content was measured. Data obtained from at least three independent experiments are expressed as means ± SE. *, #$P < 0.05$, **, ##$P < 0.01$, compared with time point 0, one-way ANOVA.

recovery of membrane D_1 receptors was achieved at 6 h in the presence of PSD-95 (Figure 6A).

This membrane receptor recovery pattern is in agreement with the results of D_1 receptor resensitization (Figure 5A). This indicates that PSD-95 shortens the time necessary for internalized D_1 receptors to return to the membrane. This conclusion is in agreement with the enhanced membrane D_1 receptor signals observed by con-

Figure 6 PSD-95 accelerates membrane D_1 receptor recovery from internalization. **(A)** HEK-293 cells stably expressing D_1 receptor were transiently transfected with mock or PSD-95. Cells were incubated with 10 μM DA at 37 °C for 1 h to induce receptor internalization (here designated as time point 0). After being washed, cells were cultured in serum-free DMEM for the indicated lengths of time (2, 6 and 15 h) and then harvested. The plasma membranes were separated and cell surface D_1 receptors were measured as described under Materials and Methods. The percentage reductions in cell surface D_1 receptors relative to untreated control are presented as the means $\pm$ SE from at least four independent experiments. **(B)** HEK-293 cells were transiently transfected with D_1-CFP, PSD-95-YFP alone or D_1-CFP + PSD-95-YFP. Thirty-six hours post transfection, cells were treated with serum-free medium for 2 h before the 1-h 10 μM DA incubation to induce D_1 receptor internalization. The cells were washed and incubated in serum-free medium for 2 or 6 h before being processed for confocal microscopy (scale bar: 50 μm). Arrows indicate large vesicles containing internalized D_1 receptors. There is no detectable autofluorescence in HEK293 cells (data not shown). **(C)** Quantification of cell surface D_1 receptors in Figure 6B. Data are presented as means $\pm$ SE from at least 20 cells for each condition. ***$P < 0.0001$ compared with the DA 1-h group using Student's paired t-test.

that PSD-95 may also speed up the spontaneous receptor recycling process of D_1 receptor (i.e., by accelerating the membrane recovery of internalized receptor). Another possibility is that PSD-95-enhanced spontaneous internalization represents a small proportion of total D_1 receptor signal because the quantified data indicate that there is no significant change in intracellular D_1 receptor levels in unstimulated cells (21.8 $\pm$ 2.9% over total D1 signal for D_1 alone; 23.7 $\pm$ 4.6% for D_1 and PSD-95 co-expression).

To examine the potential mechanism, we first tested whether PSD-95 alters D_1 receptor synthesis. RT-PCR indicated that co-transfection of PSD-95 did not alter D_1 receptor mRNA levels (data not shown). Application of the protein synthesis inhibitor cycloheximide (CHX) did not alter the rate of internalized D_1 receptor recycling in D_1 and PSD-95 co-transfected cells (Figure 7A and 7C), indicating that PSD-95-acclerated D_1 receptor recovery is not the result of enhanced D_1 receptor synthesis. However, application of monensin, a specific interrupter of the recycling pathway, blocked the enhancement of D_1 receptor recycling (Figure 7B and 7C), indicating that PSD-95-accelerated receptor recovery is most likely mediated via the facilitation of D_1 receptor recycling.
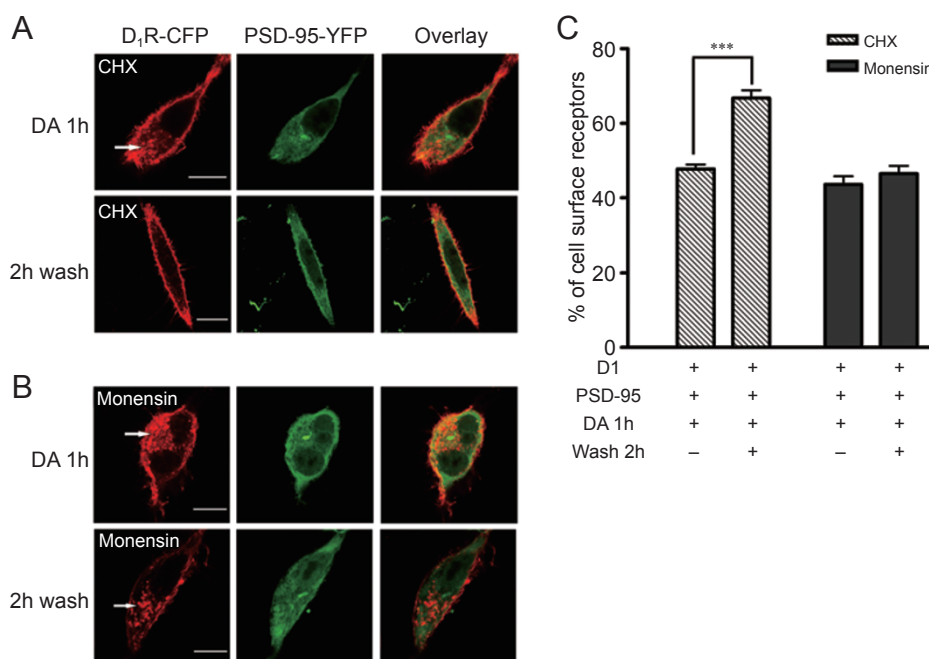
Figure 7 PSD-95 enhances D_1 receptor recycling, but not receptor synthesis. HEK-293 cells co-transfected with D_1-CFP and PSD-95-YFP were incubated with 50 μM CHX **(A)** or 50 μM monensin **(B)** in the presence of DA (10 μM for 1 h) to induce D_1 receptor internalization. After being washed, the cells were cultured in serum-free DMEM in the presence of CHX (50 μM) or monensin (50 μM) for 2 h before analysis by confocal microscopy (scale bar: 50 μm). Arrows indicate a number of vesicles containing internalized D_1 receptors. Data are representative of 10-20 independent experiments with similar results. **(C)** Quantification of surface D_1 receptors in **(A** and **B)**. Data are presented as means ± SE from 10-20 cells for each condition. ****P* < 0.0001 compared with the DA 1-h group using Student's paired *t*-test.

Discussion

The present study demonstrates that PSD-95 physically associates with D_1-like and D_2 DA receptors in HEK-293 cells that were co-transfected with PSD-95 and either D_1 or D_2 DA receptors. Stimulation of the D_1 receptor results in a transient enhanced association of the receptor with PSD-95 both *in vitro* and *in vivo*. Functional assays indicate that PSD-95 does not alter D_1 receptor-stimulated cAMP production. However, PSD-95 does accelerate recovery of the D_1 receptor to the cell membrane following the internalization of desensitized receptors that occurs during prolonged stimulation. This enhancement in receptor recycling or resensitization occurs without a significant alteration in receptor desensitization.

DA receptors play critical roles in many aspects of brain function; abnormal dopaminergic activity is closely associated with Parkinson's disease, schizophrenia, drug addiction and other neurological and psychiatric disorders [20, 21]. Like other G-protein-coupled receptors, the DA receptors are subject to internalization, desensitization and resensitization in response to agonist stimulation [1, 2]. Modulation of DA receptor trafficking has become

a focal point in attempts to understand the receptor's functional regulation. Anatomically, the D_1 DA receptors are localized in both perisynaptic and extrasynaptic areas. The present data demonstrate that the association of PSD-95 with the D_1 DA receptor is involved in D_1 receptor trafficking and consequently results in an acceleration in D_1 DA receptor resensitization. The postsynaptic area is enriched with PSD-95 [22]; PSD-95-accelerated D_1 receptor recycling and resensitization may represent a potential mechanism for the regulation of postsynaptic membrane D_1 receptors in response to the pulse release of DA from nerve terminals. Our data suggest that PSD-95 accelerates D_1 receptor recycling back to the plasma membrane, thus shortening the time of receptor recovery following receptor stimulation and subsequent internalization (Figures 6 and 7). It is thought that receptor endocytosis of desensitized GPCR is an initial step in the resensitization process that requires ligand-receptor dissociation and receptor dephosphorylation [23, 24]. Subsequently, the receptor may recycle to the membrane or be targeted for degradation [24, 25]. The recovery of receptors at the membrane has been attributed to the synthesis and insertion of more receptors, as well as to the

recycling of endocytosed receptors [25]. We found that co-transfection with PSD-95 did not alter D_1 DA receptor expression (Figure 3C), and protein synthesis inhibition did not affect PSD-95-promoted D_1 receptor recycling (Figure 7A). This suggests that PSD-95-accelerated D_1 receptor recovery is independent of new receptor synthesis. In contrast, monensin, which inhibits the recycling pathway, prevented the accelerated recovery of membrane D_1 receptors (Figure 7B), indicating that receptor recycling is the predominant mechanism involved in the PSD-95-accelerated recovery of membrane D_1 DA receptors following desensitization/internalization.

Although the underlying mechanism for PSD-95-stimulated recycling is presently unknown, it is clear that full-length PSD-95 is necessary and sufficient for accelerating D_1 DA receptor recycling. None of the truncated PSD-95 constructs, when co-expressed with the D_1 DA receptor, affected receptor resensitization (Figure 5B). Interestingly, whereas the D_1 receptor associated with PSD-95ΔSH3&GK and PSD-95ΔGK, these constructs did not affect receptor resensitization. This indicates that although physical interaction is mediated through the N-terminus, PSD-mediated resensitization requires full-length PSD-95.

A recent study has shown that PSD-95 inhibits D_1 receptor-stimulated cAMP production in HEK-293 cells co-transfected with monkey D_1 receptor and PSD-95 [18]. In contrast, we did not detect a significant change in D_1 receptor-stimulated cAMP content (Figure 3A and Table 1). Our observation is supported by results of the receptor-activated [^{35}S]GTPγS binding assay that directly assesses receptor-mediated Gs-protein activation. In this experiment, we did not find any evidence for a PSD-95-induced change in receptor-mediated Gs-protein activation in cells co-transfected with PSD-95 and D_1 receptors (Figure 3B). In fact, in some experiments we noted a slight increase in cellular cAMP production after D_1 receptor stimulation. The reason for these contradictory results is currently unknown. However, the two studies differ in the agonists used (DA/SKF38393 vs SKF81297) and receptor clones (human vs rhesus monkey D_1). These differences could underlie the discrepancy in results between the two studies.

D_1 receptor desensitization in response to agonist stimulation is believed to be associated with receptor phosphorylation, which, consequently, results in uncoupling of the D_1 DA receptor from its cognate G-protein and reduction of receptor activity [26]. Unlike a previous report showing that PSD-95 alters NMDA receptor desensitization [27], our present data demonstrate that PSD-95 elicited no change in D_1 DA receptor desensitization (Figure 4), suggesting that PSD-95 may not alter agonist-induced D_1 receptor phosphorylation.

PSD-95 is enriched in the postsynaptic area; alterations in PSD-95 were found in a number of neuropsychiatric and neurological diseases such as Alzheimer's disease, schizophrenia and Parkinson's disease. The changes in PSD-95 were suggested to be associated with altered synaptic functions [7, 8, 28, 29]. The D_1 receptor co-localizes with the NMDA receptor [30, 31] in which this interaction is critical for the formation of NMDA-mediated long-term potentiation [32, 33]. PSD-95 modulates NMDA excitatory synaptic function by directly interacting with NR2A or NR2B subunits of the NMDA receptor [34-36]. We recently reported that D_1 receptor modulation of NMDA receptor function depends on the presence of PSD-95, indicating that PSD-95 acts as an intermediate in D_1 receptor-regulated NMDA function. PSD-95 may, in turn, alter synaptic function and neuroplasticity [17]. In schizophrenia and in affective disorders, hypoactivity of NMDA receptor function and abnormal dopaminergic activity are believed to underlie the pathophysiological mechanisms. Decreased PSD-95 expression in schizophrenia has been reproducibly observed [6, 7]. It would be of great interest to study how altered PSD-95 affects the DA and NMDA receptor interaction that may ultimately result in the disruption of the neurotransmission balance in schizophrenia.

Finally, it is interesting to note that activation of the D_1 receptor resulted in a transient increase in the association between D_1 and PSD-95 both *in vitro* and *in vivo* (Figure 2B and 2C). This is of interest because it may indicate that the agonist-modulated conformation of D_1 receptor could make the receptor more accessible for PSD-95 binding. The mechanism underlying altered PSD-95 and D_1 association, as well as the pursuant functional implications is currently being studied in our laboratory.

Materials and Methods

Materials
[^{3}H]SCH23390 (specific activity 65 Ci/mmol) and [^{35}S]GTPγS (specific activity 1030 Ci/mmol) were purchased from Amersham, Inc. (Cleveland, OH, USA). The [^{125}I]cAMP assay kit was purchased from the Shanghai University of Traditional Chinese Medicine (Shanghai, PRC). DA was obtained from RBI (Natick, MA, USA). (+)-Butaclamol, isobutyl methylxanthine (IBMX), monensin and CHX were purchased from Sigma (St Louis, MO, USA). Rabbit anti-HA, anti-D_1 DA receptor, mouse anti-PSD-95, anti-c-Myc, horseradish peroxidase-linked anti-rabbit and anti-mouse secondary antibodies were purchased from Santa Cruz Biotech., Inc. (Santa Cruz, CA, USA). Other reagents were obtained as indicated in the text.

Cell culture and transfection
HEK-293 cells were maintained in Dulbecco's modified Eagle's

medium (Gibco, NY, USA) supplemented with 10% newborn calf serum (SiJiQing, Hangzhou, PRC), penicillin (100 units/ml) and streptomycin (100 units/ml). Transfections were performed when cells reached 80% confluence. For transient transfections, mock plasmids or plasmids containing the respective constructs were transfected by the calcium-phosphate method. If not specifically indicated, cells were used for experiments 24-48 h post transfection. For the selection of D_1, D_2 and D_5 receptor-expressing stable cell lines, G418 (Sigma) was added at the concentration of 300 μg/ml and was maintained at 100 μg/ml. In all experiments in which DA was applied, 100 μM L-ascorbic acid was included.

Preparations of cDNA constructs

The cDNA construct for PSD-95 was from Dr Morgan Sheng (Harvard University, Boston, MA, USA). All PSD-95 and mutant PSD-95 constructs used contained a c-Myc epitope tag inserted between residues 9 and 10 of PSD-95. Because a recent report indicated that the N terminus of PSD-95 is necessary for its association with D_1 receptor [18], all constructs made contained this N terminus. PSD-95ΔSH3&GK, PSD-95ΔGK, PSD-95ΔPDZ123 and PSD-95 cDNA-encoding fragments (as depicted by the figure depicting constructs used) were amplified by PCR from full-length cDNA clones. PSD-95, PSD-95ΔSH3&GK and PSD-95ΔGK were subcloned into pcDNA 3.0 using the *Kpn*I and *Eco*RI restriction sites. PSD-95ΔPDZ123 was subcloned into pcDNA 3.0 PSD-95-NT using the *Eco*RI and *Xho*I restriction sites. Initiation methionine residues and stop codons were also incorporated where appropriate. YFP-tagged PSD-95 was constructed by replacing the stop codon of PSD-95 complementary DNA with a *Kpn*I restriction site for in-frame fusion to the pEYFP-N1 vector. The full-length human DA D_1, D_2 and D_5 receptors cloned in pcDNA 3.1 with an HA tag at the N terminus were obtained from UMR cDNA Resource Center at University of Missouri-Rolla (Rolla, MO, USA). CFP-tagged D_1 receptor was constructed by replacing the stop codon of D_1 complementary DNA with a *Bam*HI restriction site for in-frame fusion to the pECFP-N1 vector.

Spectral fluorescence resonance energy transfer (spectral FRET) measurements

FRET signals were determined as previously described [37]. HEK-293 cells were transiently transfected with D_1 receptor in pECFP-N1 vector (D_1-CFP) and PSD-95 in pEYFP-N1 vector (PSD-95-YFP) using Lipofectamine™ 2000 (GIBCO BRL) according to the procedure recommended by the manufacturer. Fluorescence imaging was performed at room temperature 1-2 days after transfection. Immediately before fluorescence recording, the culture medium was replaced with a solution containing 130 mM NaCl, 5 mM MgCl₂, 2 mM CaCl₂, 5 mM HEPES and 1 mM EGTA (pH 7.4). Epifluorescence microscopy was carried out with a fully automated, inverted fluorescence microscope (Olympus IX-81) controlled by MetaMorph software (Universal Imaging, Inc.). Two filter sets (Chroma) were used: for CFP and FRET imaging, the filter set contained a D436/20 excitation filter and a 455dclp dichroic mirror; for YFP imaging, the filter set contained an HQ500/20 excitation filter and a Q515lp dichroic mirror. Fluorescence emission was detected with an HQ CCD camera (Hamamasu). For spectroscopic imaging, a spectrograph (Acton SpectraPro 2150i) was used in conjunction with the camera. Emission spectra specifically from the plasma membrane of the cell were collected by positioning the spectrograph slit across a cell and recording the fluorescence intensity at the position corresponding to the membrane region; the same slit position applied to both the spectrum taken with CFP excitation and the spectrum taken with YFP excitation. FRET efficiency was calculated as the enhanced YFP emission resulting from energy transfer, using an approach that was previously described [38].

Immunoprecipitation (IP) and immunoblot (IB) assay

Transfected HEK-293 cells were collected and lysed in a lysis buffer (50 mM Tris-HCl, 150 mM NaCl, 1 mM EDTA and 1% Triton X-100, pH 7.4) containing a protease inhibitor cocktail (Sigma), incubated on ice for 30 min and centrifuged at 5 000 × *g* for 10 min. The prefrontal cortex tissues were homogenized in buffer (20 mM HEPES, 150 mM NaCl, 2 mM EDTA, 10% glycerol and 0.5% NP-40, pH 7.4) and protease inhibitor cocktail, incubated on ice for 30 min and centrifuged at 20 000 × *g* for 10 min. The protein contents of the supernatants from HEK-293 cells and brain tissues were determined by bicinchoninic acid (BCA) protein assay. Aliquots of the lysate were used to detect the total expression of PSD-95 and the remainder was used for immunoprecipitation.

Aliquots of supernatant (500 μg for cells or 800 μg for tissues) were immunoprecipitated with 1 μg anti-HA (for cells expressing D_1, D_2 and D_5 receptor) or anti-D_1 receptor (for tissues) at 4 °C overnight with gentle rotation, followed by the addition of agarose-conjugated protein A/G PLUS beads (Santa Cruz Biotechnology, Santa Cruz, CA, USA) for an additional 1 h at 4 °C. To exclude the potential nonspecific pull-down, controls were included: the same amount of sample protein immunoprecipitated with non-immuno IgG; omission of the sample protein during immunoprecipitation or omission of the appropriate antibody during immunoprecipitation. The immunocomplex was then collected by centrifugation and, after samples were washed five times, the pellets were boiled in sample preparation buffer for the immunoblot assay. The immunoprecipitates or lysates were loaded onto SDS-PAGE. The proteins were separated electrophoretically and transferred to PVDF membranes (Bio-Rad). The membranes were blocked with 10% (w/v) fat-free dry milk in 0.1% Tween 20-TBS (TBST) for 2 h, followed by incubation with antibody overnight at 4 °C. The membranes were washed three times with TBST and then incubated for 1 h with species-specific HRP-conjugated secondary IgG antibody (1:5 000-1:10 000 dilution; Santa Cruz) at room temperature. The membranes were washed three times for 5 min with TBST and the signals were visualized by the ECL/HRP method (Supersignal, Pierce). The band density of D_1 receptor-associated PSD-95 was quantified by densitometry and expressed as the fold change over vehicle control.

Crude membrane preparation

Transfected HEK-293 cells were grown to confluence, washed twice with ice-cold phosphate-buffered saline (PBS), harvested with PBS and collected through centrifugation at 100 × *g* for 10 min. The cells were then lysed in hypotonic buffer (5 mM Tris-HCl and 2 mM EDTA, pH 7.4), containing a protease inhibitor mixture (Sigma) and sonicated three times for 18 s. The lysate was centrifuged at 100 × *g* for 10 min; the supernatant was further centrifuged at 40 000 × *g* for 30 min at 4 °C; the pellet was resuspended in binding buffer (50 mM Tris-HCl, 1 mM EDTA, 5 mM KCl, 1.5 mM CaCl₂, 4 mM MgCl₂ and 120 mM NaCl, pH 7.4) for

receptor-binding assays. The protein content of membranes was determined by the BCA method.

Radioligand binding assays

For radioligand saturation binding assays, the crude membrane preparation (3 μg/tube) was added to assay tubes containing 0.1 to 10 nM [^{3}H]SCH23390 in a total volume of 0.2 ml. (+)-Butaclamol was added at the final concentration of 1 μM to determine non-specific binding. After 60 min of incubation at 30 °C, the reaction was terminated by rapid filtration through a 24-well cell harvester (Brandel, Montreal, Canada) onto Whatman GF/B filters. Filters were washed with 4 ml of ice-cold washing buffer (50 mM Tris-HCl and 2 mM EDTA, pH 7.4) three times. Radioactivity bound to the filters was quantified using a Beckman LS 6500 scintillation counter. All experiments were performed in duplicate, and each experiment was repeated at least three times.

Assays of cAMP content

After 24-h transfection of plasmid-encoding D$_1$ receptor with mock, full-length or truncated PSD-95, cells were reseeded into 96-well plates (1 × 10^4 cells/well). For the assay of cAMP accumulation, cells were preincubated with 100 μl of serum-free DMEM containing 500 μM IBMX (Sigma) prior to the addition of DA at various concentrations. For receptor desensitization experiments, cells were pretreated with 10 μM DA for the indicated time and washed with serum-free DMEM before DA challenge. For receptor resensitization experiments, cells were pre-incubated with 10 μM DA for 1 h and washed, and then cells were incubated in serum-free DMEM for the indicated time before DA challenge. The reaction was then terminated on ice by the addition of 100 μl of 1 M trichloroacetic acid, followed by the addition of 20 μl 2 M K$_2$CO$_3$. The samples were centrifuged for 10 min at 3 000 × *g*. The supernatants were kept (diluted 1:50) for determining cAMP content using the [^{125}I] cAMP assay kit. All experiments were performed in duplicate and each experiment was repeated at least three times.

[^{35}S]GTPγS binding assay

Agonist-stimulated [^{35}S]GTPγS binding was performed in reaction buffer containing 50 mM Tris, 5 mM MgCl$_2$, 1 mM EDTA, 100 mM NaCl and 1 mM DTT, pH 7.4. The assay mixture (200 μl) contained 15 μg of crude membrane protein, 0.1 nM [^{35}S]GTPγS and 20 μM GDP (Sigma) in the absence or presence of various concentrations of DA. The reaction was stopped after 10 min of incubation at 30 °C with 3 ml of ice-cold reaction buffer. Samples were filtered rapidly through a GF/B filter and rinsed three times with 3 ml of reaction buffer. Filters were dried and the binding activity was measured by liquid scintillation counting. Nonspecific binding was detected in the presence of 100 μM unlabeled GTPγS (Sigma).

Measurement of cell surface receptors

Crude cell membranes were prepared as described above. The heavy membrane fraction and the light vesicular membrane were separated using a method described by Lamey *et al.* [39]. Briefly, crude membranes were resuspended in hypotonic buffer (5 mM Tris-HCl and 2 mM EDTA, pH 7.4) with protease inhibitor mixture, layered on top of a 35% sucrose cushion, and then centrifuged at 150 000 × *g* for 90 min at 4 °C. The heavy membrane

fractions at the bottom of the sucrose cushion were resuspended in binding buffer and the protein contents were determined by the BCA method and adjusted (10 μg/tube) for radioligand binding assays using 1.2 nM [^{3}H]SCH23390 (0.9 K_d) to evaluate the density of membrane receptors.

Confocal microscopy and image quantification

Cells expressing D$_1$-CFP with or without co-expression of PSD-95-YFP were treated either with 10 μM DA or vehicle for the indicated time in serum-free DMEM and then washed three times with ice-cold PBS to stop the reaction. For assays of cell surface receptor recovery, cells were rinsed once with PBS and then incubated in serum-free DMEM for 2 or 6 h followed by treatment with 10 μM DA or vehicle for 1 h. The cells were then fixed in 4% paraformaldehyde for 20 min at room temperature prior to three washes with PBS. Recovery of the receptor was then observed with a Leica SP2 confocal microscope. For quantifying the ratio of cell-surface D$_1$ receptor signal to whole-cell D$_1$ receptor signal, the D$_1$ receptor fluorescence intensities for whole cell and for intracellular signal were measured for each cell. The ratio of cell surface D$_1$ receptors was defined as (1 – intracellular/total cellular fluorescence) × 100%.

Data analysis

The radioligand binding parameters K_d and B_{max}, as well as the EC$_{50}$ and E_{max} values for DA-stimulated cAMP production were fitted and calculated using the Prism program (GraphPad Software, San Diego, CA, USA). The curves presented in this paper represent the best fits to the data. Data were expressed as the means ± SE. Significance was considered at the $P < 0.05$ level using Student's paired *t*-test or one-way ANOVA. Semi-quantification of immunoblot signals was performed by scanning the films and analysis was performed using NIH Image software.

Acknowledgments

References

1   Ng GY, Trogadis J, Stevens J, Bouvier M, O'Dowd BF, George SR. Agonist-induced desensitization of dopamine D1 receptor-stimulated adenylyl cyclase activity is temporally and biochemically separated from D1 receptor internalization. *Proc Natl Acad Sci USA* 1995; **92**:10157-10161.
2   Barton AC, Sibley DR. Agonist-induced desensitization of D1-dopamine receptors linked to adenylyl cyclase activity in cultured NS20Y neuroblastoma cells. *Mol Pharmacol* 1990;

38:531-541.

3 Dumartin B, Caille I, Gonon F, Bloch B. Internalization of D1 dopamine receptor in striatal neurons *in vivo* as evidence of activation by dopamine agonists. *J Neurosci* 1998; **18**:1650-1661.

4 Kennedy MB. Signal-processing machines at the postsynaptic density. *Science* 2000; **290**:750-754.

5 Sierralta J, Mendoza C. PDZ-containing proteins: alternative splicing as a source of functional diversity. *Brain Res Rev* 2004; **47**:105-115.

6 Toro C, Deakin JF. NMDA receptor subunit NRI and postsynaptic protein PSD-95 in hippocampus and orbitofrontal cortex in schizophrenia and mood disorder. *Schizophr Res* 2005; **80**:323-330.

7 Kristiansen LV, Meador-Woodruff JH. Abnormal striatal expression of transcripts encoding NMDA interacting PSD proteins in schizophrenia, bipolar disorder and major depression. *Schizophr Res* 2005; **78**:87-93.

8 Kristiansen LV, Beneyto M, Haroutunian V, Meador-Woodruff JH. Changes in NMDA receptor subunits and interacting PSD proteins in dorsolateral prefrontal and anterior cingulate cortex indicate abnormal regional expression in schizophrenia. *Mol Psychiatry* 2006; **11**:737-747, 705.

9 Kim E, Sheng M. PDZ domain proteins of synapses. *Nat Rev Neurosci* 2004; **5**:771-781.

10 Iwamoto T, Yamada Y, Hori K, Watanabe Y, Sobue K, Inui M. Differential modulation of NR1-NR2A and NR1-NR2B subtypes of NMDA receptor by PDZ domain-containing proteins. *J Neurochem* 2004; **89**:100-108.

11 Bockaert J, Fagni L, Dumuis A, Marin P. GPCR interacting proteins (GIP). *Pharmacol Ther* 2004; **103**:203-221.

12 Garner CC, Nash J, Huganir RL. PDZ domains in synapse assembly and signalling. *Trends Cell Biol* 2000; **10**:274-280.

13 Funke L, Dakoji S, Bredt DS. Membrane-associated guanylate kinases regulate adhesion and plasticity at cell junctions. *Annu Rev Biochem* 2005; **74**:219-245.

14 Craven SE, Bredt DS. PDZ proteins organize synaptic signaling pathways. *Cell* 1998; **93**:495-498.

15 Kornau HC, Seeburg PH, Kennedy MB. Interaction of ion channels and receptors with PDZ domain proteins. *Curr Opin Neurobiol* 1997; **7**:368-373.

16 Sheng M, Sala C. PDZ domains and the organization of supra-molecular complexes. *Annu Rev Neurosci* 2001; **24**:1-29.

17 Gu WH, Yang S, Shi WX, Jin GZ, Zhen XC. Requirement of PSD-95 for dopamine D1 receptor modulating glutamate NR1a/NR2B receptor function. *Acta Pharmacol Sin* 2007; **28**:756-762.

18 Zhang J, Vinuela A, Neely MH, *et al*. Inhibition of the dopamine D1 receptor signaling by PSD-95. *J Biol Chem* 2007; **282**:15778-15789.

19 O'Dowd BF, Ji X, Alijaniaram M, *et al*. Dopamine receptor oligomerization visualized in living cells. *J Biol Chem* 2005; **280**:37225-37235.

20 Jaber M, Robinson SW, Missale C, Caron MG. Dopamine receptors and brain function. *Neuropharmacology* 1996; **35**:1503-1519.

21 Missale C, Nash SR, Robinson SW, Jaber M, Caron MG. Dopamine receptors: from structure to function. *Physiol Rev* 1998; **78**:189-225.

22 Cho KO, Hunt CA, Kennedy MB. The rat brain postsynaptic density fraction contains a homolog of the Drosophila discs-large tumor suppressor protein. *Neuron* 1992; **9**:929-942.

23 Trincavelli ML, Tuscano D, Cecchetti P, *et al*. Agonist-induced internalization and recycling of the human A$_3$ adenosine receptors: role in receptor desensitization and resensitization. *J Neurochem* 2000; **75**:1493-1501.

24 Zhang J, Ferguson SS, Barak LS, *et al*. Molecular mechanisms of G protein-coupled receptor signaling: role of G protein-coupled receptor kinases and arrestins in receptor desensitization and resensitization. *Receptors Channels* 1997; **5**:193-199.

25 Martin-Negrier ML, Charron G, Bloch B. Receptor recycling mediates plasma membrane recovery of dopamine D1 receptors in dendrites and axons after agonist-induced endocytosis in primary cultures of striatal neurons. *Synapse* 2006; **60**:194-204.

26 Gardner B, Liu ZF, Jiang D, Sibley DR. The role of phosphorylation/dephosphorylation in agonist-induced desensitization of D1 dopamine receptor function: evidence for a novel pathway for receptor dephosphorylation. *Mol Pharmacol* 2001; **59**:310-321.

27 Li B, Otsu Y, Murphy TH, Raymond LA. Developmental decrease in NMDA receptor desensitization associated with shift to synapse and interaction with postsynaptic density-95. *J Neurosci* 2003; **23**:11244-11254.

28 Gylys KH, Fein JA, Yang F, Wiley DJ, Miller CA, Cole GM. Synaptic changes in Alzheimer's disease: increased amyloid-beta and gliosis in surviving terminals is accompanied by decreased PSD-95 fluorescence. *Am J Pathol* 2004; **165**:1809-1817.

29 Nash JE, Johnston TH, Collingridge GL, Garner CC, Brotchie JM. Subcellular redistribution of the synapse-associated proteins PSD-95 and SAP97 in animal models of Parkinson's disease and L-DOPA-induced dyskinesia. *FASEB J* 2005; **19**:583-585.

30 Fiorentini C, Gardoni F, Spano P, Di Luca M, Missale C. Regulation of dopamine D1 receptor trafficking and desensitization by oligomerization with glutamate N-methyl-D-aspartate receptors. *J Biol Chem* 2003; **278**:20196-20202.

31 Lee FJ, Xue S, Pei L, *et al*. Dual regulation of NMDA receptor functions by direct protein-protein interactions with the dopamine D1 receptor. *Cell* 2002; **111**:219-230.

32 Calabresi P, Gubellini P, Picconi B, *et al*. Inhibition of mitochondrial complex II induces a long-term potentiation of NMDA-mediated synaptic excitation in the striatum requiring endogenous dopamine. *J Neurosci* 2001; **21**:5110-5120.

33 Fiorentini C, Missale C. Oligomeric assembly of dopamine D1 and glutamate NMDA receptors: molecular mechanisms and functional implications. *Biochem Soc Trans* 2004; **32**:1025-1028.

34 Kornau HC, Schenker LT, Kennedy MB, Seeburg PH. Domain interaction between NMDA receptor subunits and the postsynaptic density protein PSD-95. *Science* 1995; **269**:1737-1740.

35 Kim E, Cho KO, Rothschild A, Sheng M. Heteromultimerization and NMDA receptor-clustering activity of Chapsyn-110, a member of the PSD-95 family of proteins. *Neuron* 1996; **17**:103-113.

36 Niethammer M, Kim E, Sheng M. Interaction between the C terminus of NMDA receptor subunits and multiple members of

the PSD-95 family of membrane-associated guanylate kinases. *J Neurosci* 1996; **16**:2157-2163.

37 Cheng W, Yang F, Takanishi CL, Zheng J. Thermosensitive TRPV channel subunits coassemble into heteromeric channels with intermediate conductance and gating properties. *J Gen Physiol* 2007; **129**:191-207.

38 Takanishi CL, Bykova EA, Cheng W, Zheng J. GFP-based FRET analysis in live cells. *Brain Res* 2006; **1091**:132-139.

39 Lamey M, Thompson M, Varghese G, *et al.* Distinct residues in the carboxyl tail mediate agonist-induced desensitization and internalization of the human dopamine D1 receptor. *J Biol Chem* 2002; **277**:9415-9421.